A&A 492, 875–881 (2008)
DOI: 10.1051/0004-6361:200810589

Astronomy & Astrophysics

Accurate rest frequencies for the submillimetre-wave lines of C_3O in ground and vibrationally excited states below 400 cm^{-1} [⋆]

L. Bizzocchi, C. Degli Esposti, and L. Dore

Dipartimento di Chimica "G. Ciamician", via F. Selmi 2, 40126 Bologna, Italy
e-mail: `[luca.bizzocchi;claudio.degliesposti;luca.dore]@unibo.it`

Received 14 July 2008 / Accepted 18 September 2008

ABSTRACT

The submillimetre-wave spectrum of C_3O ($X^1\Sigma^+$) has been investigated in the laboratory using a source-modulation microwave spectrometer equipped with a gas-phase flow pyrolysis system for the production of unstable chemical species. C_3O was produced by thermal decomposition of fumaryl chloride at 900 °C. Thirty-seven new rotational transitions were observed in the frequency range 307–740 GHz for the ground vibrational state, reaching a J quantum number as high as 76. Additionally, new millimetre-wave and submillimetre-wave lines were recorded for the bending fundamental $\upsilon_5 = 1$, and for its overtones $\upsilon_5 = 2$ and $\upsilon_5 = 3$ whose rotational spectra have been identified for the first time. The new laboratory measurements provide much improved rest frequencies in the submillimetre spectral region for the ground state spectra of C_3O, and for the first levels of its low-energy υ_5 vibrational ladder, useful for the radioastronomical identification of their rotational lines in the ISM.

Key words. molecular data – methods: laboratory – techniques: spectroscopic – radio lines: ISM

1. Introduction

Tricarbon monoxide (C_3O) is the longest oxygen-containing carbon chain observed in the interstellar medium (ISM). It was first identified by Matthews et al. (1984) through its $J = 2$–1 rotational line in the molecular cloud TMC-1 toward the cyanopolyyne peak, shortly after its first laboratory study (Brown et al. 1983). Recently, C_3O has been detected towards the carbon star IRC+10216 (Tenenbaum et al. 2006) together with other O-bearing species, such as H_2O (Melnick et al. 2001; Hasegawa et al. 2006), OH (Ford et al. 2003) and H_2CO (Ford et al. 2004). This object is an evolved low-mass AGB star whose mass loss produces a dusty, molecular-rich, extended envelope. The dredge-up process has altered the elemental C/O ratio of the star surface (which is $C/O < 1$ during the main sequence phase), resulting in a strong carbon enrichment which ultimately determines the kind of chemistry taking place in the inner envelope (Tsuji 1973): in these conditions, the bulk of oxygen in IRC+10216 is expected to be locked into the highly stable CO molecule.

The existence of other O-bearing species in IRC+10216 has been interpreted as the results of water ice evaporation from orbiting Kuiper belt-type objects (Melnick et al. 2001), or alternatively it has been supposed that gas-phase oxygen-rich chemistry, involving neutral-neutral reactions, occurs in the outer shell of the star (Tenenbaum et al. 2006; Agúndez & Cernicharo 2006). Also, in a very recent study, Palumbo et al. (2008) have suggested that in dense molecular clouds, where high CO depletion occurs, significant amounts of carbon chain oxides, C_nO, might be formed in the solid phase after cosmic ion irradiation of CO-rich dust grains, and then released to the gas phase when desorption of icy mantles takes place. This remains however an open question due to the paucity of observational data on carbon chain oxides.

In the laboratory, C_3O has been the subject of various spectroscopic investigations: after the first identification of its centimetre-wave (cm-wave) spectrum (Brown et al. 1983), the same authors performed a detailed microwave study on isotopic species, leading to a structure determination (Brown et al. 1985). Later, its ground-state millimetre-wave (mm-wave) spectrum was also recorded (Tang et al. 1985; Klebsch et al. 1985), and a high-resolution infrared study of the ν_1 and some associated hot bands has been performed using Fourier transform infrared spectroscopy (FTIR) (McNaughton et al. 1991).

Presently, the best set of rotational and centrifugal distortion constants are those provided by the mm-wave study of Klebsch et al. (1985), which indeed allow the calculation of reliable rest-frequencies for the ground state lines of C_3O at millimetre wavelengths. However, it should be noted that C_3O is a molecule with a certain degree of floppiness (Botschwina 2005), which results in relatively large centrifugal distortion effects. Hence, the extrapolation of the high-J submillimetre-wave (submm-wave) line positions from lower frequency laboratory measurements may be inaccurate, and the corresponding predicted uncertainties are likely to be misleadingly underestimated.

As regards the vibrationally excited states, the spectroscopic information is much more scarce. Few low-J rotational lines of the $\upsilon_5 = 1$ bending state were recorded by Brown et al. (1985), while for the $\upsilon_5 = 2$ and $\upsilon_5 = 3$ overtone states the only available spectroscopic data are those derived from the rovibrational band-by-band analysis of the ν_1 hot band system (McNaughton et al. 1991). The ν_5 bending mode of C_3O has an energy of 114 cm^{-1} (Hochlaf 2001), thus the first members of its vibrational ladder might be populated by the radiative pumping mechanism occurring in IRC+10216, which is one of the brightest objects of

---

[⋆] Tables 5 to 8 are only available in electronic form at the CDS via anonymous ftp to `cdsarc.u-strasbg.fr (130.79.128.5)` or via `http://cdsweb.u-strasbg.fr/cgi-bin/qcat?J/A+A/492/875`

Article published by EDP Sciences

the infrared sky. In this object, several molecules in vibrationally excited states have already been detected, including the carbon chains C_3H, C_4H, and HC_3N (Cernicharo et al. 2000). The detection of vibrationally excited C_3O may provide additional clues to understanding oxygen chemistry in C-rich circumstellar envelopes, and for this the availability of reliable rest frequencies is a prime prerequisite.

The accuracy of the spectral data on astrophysically important molecules will become even more critical in the near future, when the ongoing HERSCHEL and ALMA projects will reach their full operating status. New perspectives in astrophysical spectroscopy will be provided by the extended spectral coverage of the HIFI spectrometer (onboard HERSCHEL) and by the unprecedented sensitivity and angular resolution of ALMA, whose very small beam sizes can be exploited to selectively study the densest and most excited regions. In this context, the availability of very accurate rest frequencies, ideally obtained by direct laboratory measurements, is highly desirable both for the unambiguous identification of the molecular signals and also for modelling purposes.

The aim of the present investigation is to provide improved rotational spectral data to assist the the mm-wave and submm-wave radioastronomical searches of C_3O in its ground and lowest vibrationally excited states. New laboratory measurements of the ground state C_3O spectrum have been carried out reaching a frequency as high as 739 GHz: thirty-seven new rotational transitions from $J = 32$–31 to $J = 77$–76 have been recorded and analysed, yielding much improved values of the rotational constant B and of the quartic and sextic centrifugal distortion constants D and H. Moreover, the octic L constant, of the order of J^8, had to be included in the analysis in order to take into account the large centrifugal distortion effects exhibited by the C_3O molecule. New mm-wave and submm-wave rotational lines spanning the J range 7–59 (frequency interval 77–580 GHz) have also been recorded for the lowest fundamental $v_5 = 1$, and for its overtones $v_5 = 2$ and $v_5 = 3$. These transition frequencies have been analysed employing a model Hamiltonian that takes into account the l-type resonance effects arising between different sublevels of a given bending state as well as their centrifugal corrections. The resulting set of spectroscopic constants allows for the prediction of the rotational line positions of C_3O, with an uncertainty of few thousandths of km s^{-1} up to 1 THz for the ground state lines and up to 600 GHz for the bending excited state spectra.

2. Experiment

In previous laboratory investigations the C_3O molecule was produced either by glow discharge of carbon suboxide, C_3O_2, (Tang et al. 1985) or by pyrolytic processes, employing various stable precursors (Brown et al. 1983; Klebsch et al. 1985; Brown et al. 1985; McNaughton et al. 1991). In the present investigation we found it convenient to produce C_3O by flow-pyrolysis of fumaryl chloride (Aldrich), using the same apparatus already employed to generate HC_5N (Yamada et al. 2004) and HC_7N (Bizzocchi & Degli Esposti 2004). Briefly, vapours of the precursor were flowed through a quartz tube, 50 cm long and 1 cm in diameter, whose central part was heated at 900 °C by a 30 cm long cylindrical furnace. The high-temperature reactor was connected to the absorption cell of the spectrometer and the C_3O spectra were recorded while continuously pumping the pyrolysis products through the system. The pyrolysis reaction scheme is:

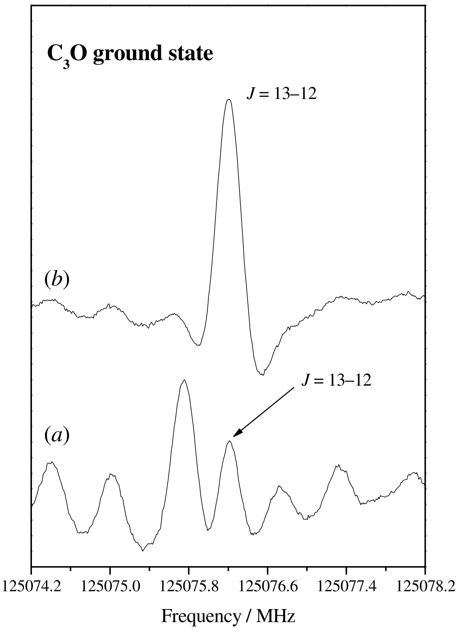

Fig. 1. Recordings of the $J = 13$–12 rotational transition of C_3O in its ground vibrational state obtained by **a)** pyrolysis of pure fumaryl chloride vapours and **b)** copyrolysis of a 2:1 mixture of fumaryl chloride and methyl acetylene. The reaction temperature was 900 °C.

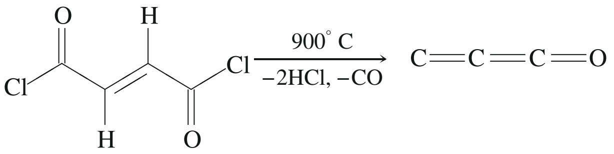

In our experimental conditions, C_3O has proven to be a quite unstable species with a lifetime of the order of 1 s, thus a high flow rate in the pyrolysis system and in the absorption cell was critical to achieve sufficiently strong spectral features. During the measurements we noticed that the addition of 50% methyl acetylene (CH_3CCH) to the precursor vapours produced a significative enhancement of the C_3O absorption signals, as well as a substantial reduction of the intensity of the interfering lines. This beneficial effect is well illustrated in Fig. 1 which shows recordings of the ground state $J = 13$–12 transition of C_3O produced pyrolysing pure fumaryl chloride (lower trace) and a 2:1 mixture of fumaryl chloride and CH_3CCH (upper trace). Typically, 100 mTorr (13 Pa) of fumaryl chloride vapours and 50 mTorr (7 Pa) of CH_3CCH were flowed into the quartz reactor corresponding to a total pressure of ca. 12 mTorr (≈2 Pa) inside the absorption cell.

However, even in the best conditions, the recorded spectra were very often contaminated by several interfering lines produced by the unreacted precursors and by the various side products of the pyrolysis process, the most prominent of which are chloroacetylene, chlorodiacetylene, and 2-propynoyl chloride (McNaughton et al. 1991). These features are in general weaker than the most intense C_3O lines, but they are still a considerable drawback when the faint spectra of the vibrationally excited states are sought for. This problem may be overcome by taking advantage of the instability of the C_3O molecule, whose lifetime is shorter than that of most of the contaminating byproducts. If the pyrolysed mixture is trapped in the absorption

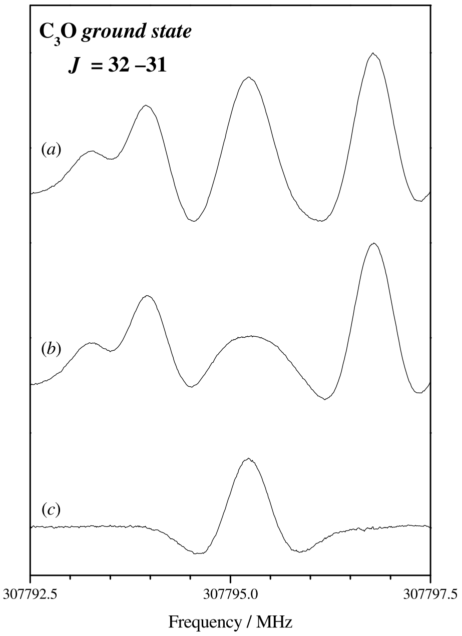

Fig. 2. Recordings of the rotational spectrum of C_3O in the region of the $J = 32$–31 transition of the ground vibrational state. Trace **a)**: flow copyrolysis of fumaryl chloride and methyl acetylene 2:1 mixture at 900 °C, cell pressure 12 mTorr (1.6 Pa). Trace **b)**: static sample of the pyrolysis products, cell pressure 12 mTorr (1.6 Pa). Trace **c)**: difference.

cell, the signals of C_3O quickly disappear while the intensity of the interfering lines remains nearly unchanged. The "trapping" can be easily achieved by first choking the valve of the pumping system, and then closing the precursors metering valves. A slow pumping through the choked valve is allowed until the pressure of the absorption cell has redescended to the typical flow value (≈2 Pa), and at this point the output valve is definitively closed leaving a static sample of pyrolysis products inside the cell. By taking the difference between the spectrum recorded under flowing conditions and that recorded with the static sample, it is possible to attain a nearly complete cancellation of the lines due to stable molecules, thus obtaining a much cleaner spectrum of C_3O. An example of this method is presented in Fig. 2, which shows the recording of the ground state $J = 32$–31 transition: the three interfering features existing in the flowing sample (trace a) completely vanish in the difference spectrum (trace c), resulting in a flat baseline and in a cleaner absorption profile of the relevant line.

Measurements were performed in the frequency range 75–740 GHz employing phase-locked Gunn oscillators (Carlstrom and RPG) as primary radiation sources working in the frequency range 75–115 GHz; power at submillimetre wavelengths was obtained using harmonic multiplication. Source frequency modulation at 16.7 kHz was applied and the signal was demodulated at $2f$ by a lock-in amplifier, thus obtaining the second derivative of the actual spectrum profile. A Schottky-barrier diode (Millitech) and a liquid-He-cooled InSb detector (QMC) were used to record the spectra below and above 190 GHz respectively. Measurement accuracy of the line positions lies in the range 10–20 kHz, depending on the signal-to-noise ratio.

3. Observed spectra and analysis

We have investigated the mm-wave and submm-wave spectra of C_3O in the ground state and in the $v_5 = 1$, $v_5 = 2$, and $v_5 = 3$ bending excited states, which all lie below 400 cm^{-1} (Hochlaf 2001). An earlier set of cm-wave and mm-wave frequency data was available for the vibrational ground state (see Klebsch et al. 1985, and references therein), for which we have extended the measurements reaching a frequency as high as 739 GHz.

As far as excited states are concerned, few low frequency lines had been recorded for the $v_5 = 1$ bending state, while no spectroscopic data were available for its overtones $v_5 = 2$ and $v_5 = 3$. For these vibrationally excited states we carried out new measurements in the 77–580 GHz frequency interval and, since they involve excitation of the v_5 bending quantum, multiplets of rotational lines were always recorded for each $J + 1 \leftarrow J$ transition, owing to l-type resonance effects between the different l sublevels.

The spectra were analysed using the formalism originally developed by Yamada and coworkers (Yamada et al. 1985; Niederhoff & Yamada 1993) and already employed to fit the excited-state rotational spectra of the astrophysically important carbon chains HC_5N (Yamada et al. 2004) and HC_7N (Bizzocchi & Degli Esposti 2004). Briefly, the ro-vibrational Hamiltonian was first represented using the unsymmetrised basis functions $|v_5, l_5; J\rangle$, thus obtaining an energy matrix whose diagonal elements have the form:

$$\begin{aligned}\langle v_5, l_5; J|\,\hat{H}\,|v_5, l_5; J\rangle \;=\; & x_{L(5,5)} l_5^2 + \left(B_v + \mathrm{d}_{JL(5,5)} l_5^2\right) \\ & \times \left[J(J+1) - l_5^2\right] \\ & - \left(D_v + h_{JL(5,5)} l_5^2\right)\left[J(J+1) - l_5^2\right]^2 \\ & + H_v\left[J(J+1) - l_5^2\right]^3 \\ & + L_v\left[J(J+1) - l_5^2\right]^4, \qquad (1)\end{aligned}$$

whereas off-diagonal ($\Delta l_5 = \pm 2$), l-type resonance terms are given by:

$$\begin{aligned}\langle v_5, l_5 \pm 2; J|\,\hat{H}\,|v_5, l_5; J\rangle = & \frac{1}{4}\left[q_5 + q_{5J} J(J+1) + q_{5JJ} J^2(J+1)^2\right] \\ & \times \sqrt{(v_5 \mp l_5)\,(v_5 \pm l_5 + 2)} \\ & \times \sqrt{[J(J+1) - l_5(l_5 \pm 1)]\,[J(J+1) - (l_5 \pm 1)(l_5 \pm 2)]}. \qquad (2)\end{aligned}$$

The resulting energy matrix has been then factorised in symmetric and antisymmetric blocks adopting Wang-type linear combinations of wavefunctions (Yamada et al. 1985). Any sublevel belonging to a given vibrational state can therefore be labelled through its l_5 value and by the "+" or "−" superscripts which designate which kind of symmetrised linear combination of wavefunctions has been chosen. Over 180 new transition frequencies have been measured, and some details dealing with the analyses performed for the various vibrational states investigated are given in the following subsections.

3.1. The ground state

The previous investigations of the ground-state rotational spectra of C_3O cover the frequency interval almost continuously between 9 and 206 GHz, plus two isolated recordings at 300 and 375 GHz. We measured 37 new rotational transitions in the frequency range 307–740 GHz spanning J values from 31 to 76.

Table 1. Analysed transition frequencies and least-squares residuals (MHz) for C_3O in the vibrational ground state.

Transition	Observed	Obs. – Calc.	Transition	Observed	Obs. – Calc.
1–0	9621.762^{a}	–0.008	38–37	375 065.845^{d}	0.007
2–1	19 243.531^{a}	0.010	40–39	384 673.215	–0.006
3–2	28 865.227^{a}	–0.007	41–40	394 279.878	0.002
4–3	38 486.862^{a}	–0.030	42–41	403 885.778	–0.008
5–4	48 108.504^{a}	0.029	43–42	413 490.938	0.005
6–5	57 729.962^{a}	–0.003	44–43	423 095.307	0.006
7–6	67 351.345^{b}	0.003	50–49	480 704.196	0.019
8–7	76 972.582^{b}	–0.007	51–50	490 302.613	0.002
9–8	86 593.678^{b}	–0.009	52–51	499 900.133	0.002
10–9	96 214.619^{b}	0.003	53–52	509 496.724	0.005
11–10	105 835.363^{b}	0.003	54–53	519 092.368	0.008
12–11	115 455.899^{b}	0.001	55–54	528 687.035	–0.003
13–12	125 076.212^{b}	0.000	56–55	538 280.736	0.002
14–13	134 696.282^{b}	–0.003	57–56	547 873.422	–0.013
15–14	144 316.098^{c}	0.001	58–57	557 465.113	–0.009
16–15	153 935.639^{c}	0.010	59–58	567 055.754	–0.027
17–16	163 554.868^{b}	0.004	60–59	576 645.383	–0.012
18–17	173 173.799^{c}	0.016	61–60	586 233.922	–0.027
19–18	182 792.354^{b}	–0.014	62–61	595 821.435	0.010
22–21	211 645.924^{c}	–0.007	63–62	605 407.835	0.026
23–22	221 262.992^{c}	–0.002	64–63	614 993.098	0.013
24–23	230 879.625^{c}	–0.007	65–64	624 577.239	0.002
27–26	259 726.819^{c}	0.011	66–65	634 160.259	0.010
31–30	298 182.646^{c}	–0.003	67–66	643 742.117	0.011
32–31	307 795.228	0.000	68–67	653 322.803	0.011
33–32	317 407.217	–0.003	69–68	662 902.291	–0.002
34–33	327 018.606	–0.001	70–69	672 480.574	–0.018
35–34	336 629.366	–0.004	71–70	682 057.668	–0.006
36–35	346 239.489	–0.003	75–74	720 353.535	0.001
37–36	355 848.955	–0.001	76–75	729 924.299	–0.007
39–38	365 457.744	0.001	77–76	739 493.777	0.006

Notes – Assumed uncertainties are 20 kHz for all the transitions. ^{a} From Brown et al. (1983); ^{b} from Brown et al. (1985); ^{c} from Klebsch et al. (1985); ^{d} mean value of the measurement of Klebsch et al. (1985) and the present work.

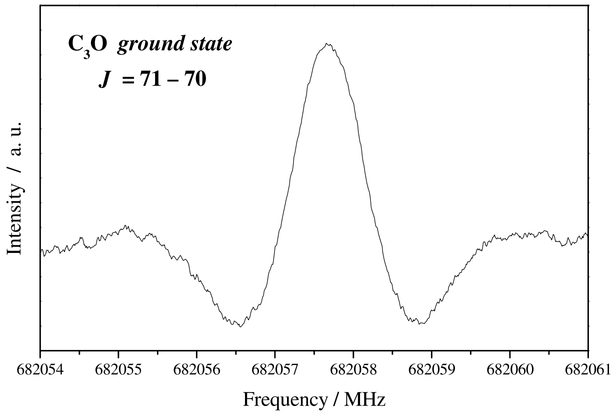

Fig. 3. Recording of the $J = 71$–70 rotational transition of C_3O in its ground vibrational state. Twenty-four scans with a time constant of 30 ms have been coadded (total integration time 58 s).

Figure 3 presents the recording of the $J = 71$–70 transition at 682 GHz. The submm-wave lines were readily identified on the basis of the spectroscopic parameters of Klebsch et al. (1985), but systematic low-frequency displacements from the predicted positions were observed for high-J transitions, reaching a maximum deviation of –3.2 MHz for $J = 77$–76. These new frequencies were analysed through Eq. (1) (with $l_5 = 0$) including in the data set all the previously available data (Brown et al. 1983, 1985; Tang et al. 1985; Klebsch et al. 1985) with equal weighting. The complete list of the transition frequencies analysed and of the corresponding least-squares residuals are reported in Table 1. The fit yielded improved values of the rotational constant B and of the centrifugal distortion constants D and H, as well as a novel value of the octic centrifugal distortion constant L which was determined with an uncertainty of about 3%. The results of the least-squares fit are reported in the first column of Table 2.

3.2. The bending excited states $v_5 = 1$, $v_5 = 2$ and $v_5 = 3$

A few cm-wave lines for the $\upsilon_5 = 1$ excited state were measured by Brown et al. (1985), while no previous information was available for the pure rotational spectra of the $\upsilon_5 = 2$ and $\upsilon_5 = 3$ bending overtones. Owing to the l-type resonance effects, each $J + 1 \leftarrow J$ transition of $\upsilon_5 = 1$ is split into a doublet (l-type doubling), whereas the $\upsilon_5 = 2$ and $\upsilon_5 = 3$ lines are split into a triplet and a quadruplet of components, respectively. From ab initio calculations (Hochlaf 2001; Botschwina 2005) their vibrational energy can be estimated to be about 230 cm^{-1} and 340 cm^{-1}, thus the 300 K peak intensity of their transitions is expected to be 1/3 and 1/5 of the corresponding ground state lines. At this level of intensity, the spectral congestion was very high and the method described in the Experiment section proved to be crucial for the identification and assignment of the line multiplets belonging to the $\upsilon_5 = 2$ and $\upsilon_5 = 3$ states.

Measurements were performed in the 77–581 GHz frequency range, reaching a J value as high as 59 for $\upsilon_5 = 1$, and 40

Table 2. Spectroscopic constants determined for the ground and $\upsilon_5 = 1$, $\upsilon_5 = 2$, and $\upsilon_5 = 3$ bending excited states of C_3O.

		Ground state	$\upsilon_5 = 1$	$\upsilon_5 = 2$	$\upsilon_5 = 3$
B	/ MHz	4810.88641(10)	4848.67340(13)	4886.27982(21)	4923.65763(15)
D	/ kHz	0.778342(63)	1.009944(62)	1.23930(15)	1.46451(13)
H	/ mHz	2.606(14)	4.9141(90)	7.274(49)	9.582(40)
L	/μHz	–0.0289(10)	–0.0289^a	–0.0289^a	–0.0289^a
q_5	/ MHz		13.54402(24)	13.69251^a	13.84101(12)
q_{5J}	/ kHz		–0.15169(12)	–0.15482^a	–0.157964(47)
q_{5JJ}	/ mHz		2.245(18)	2.245^a	2.245^a
$x_{L(5,5)}$	/ GHz			26.10176(27)	25.65977(72)
$d_{JL(5,5)}$	/ kHz		–69.151^a	–66.048(59)	–62.945(24)
$h_{JL(5,5)}$	/ Hz		2.895^a	2.656(22)	2.417(12)
$\sigma_{\rm fit}$	/ kHz	11.2	16.2	10.2	9.4
no. of lines		62	59	39	48
J range		0–76	1–59	8–40	8–40

Notes. – Standard errors in units of the last digit are given in parentheses for the fitted parameters. ^{a} Fixed in the analysis.

Table 3. Analysed transition frequencies and least-squares residuals (MHz) for C_3O in the $\upsilon_5 = 1$ vibrationally excited state.

Transition	Observed	Obs. – Calc.	σ^a	Observed	Obs. – Calc.	σ^a
	$l_5 = 1^-$			$l_5 = 1^+$		
2–1	19 367.345^b	0.038	0.100	19 421.465^b	–0.013	0.100
3–2	29 050.903^b	–0.002	0.100	29 132.134^b	–0.019	0.100
4–3	38 734.412^b	–0.024	0.100	38 842.747^b	–0.002	0.100
5–4	48 417.894^b	0.017	0.100	48 553.282^b	0.041	0.100
8–7	77 467.464	0.023	0.020	77 683.847	0.011	0.020
9–8	87 150.299	–0.003	0.020	87 393.645	–0.008	0.020
10–9	96 832.979	0.017	0.020	97 103.239	0.002	0.020
11–10	106 515.397	–0.002	0.020			
12–11	116 197.596	0.005	0.020	116 521.624	0.022	0.020
13–12	125 879.533	0.018	0.020	126 230.307	–0.025	0.020
14–13			0.020	135 938.755	0.030	0.020
15–14	145 242.484	0.011	0.020	145 646.770	0.014	0.020
17–16	164 604.088	–0.008	0.020			
18–17			0.020	174 768.436	0.012	0.020
21–20			0.020	203 885.933	0.013	0.020
26–25	251 710.165	–0.016	0.020	252 403.962	–0.004	0.020
35–34	338 769.871	–0.002	0.020	339 692.624	–0.024	0.020
36–35	348 439.627	–0.008	0.020	349 387.297	–0.014	0.020
37–36	358 108.599	–0.015	0.020	359 081.055	–0.017	0.020
38–37	367 776.772	–0.016	0.020	368 773.902	–0.005	0.020
39–38	377 444.135	–0.001	0.020	378 465.787	–0.007	0.020
40–39	387 110.639	–0.000	0.020	388 156.714	0.005	0.020
41–40	396 776.279	0.002	0.020	397 846.615	–0.015	0.020
42–41	406 441.034	0.006	0.020	407 535.526	–0.008	0.020
43–42	416 104.882	0.009	0.020	417 223.400	0.001	0.020
44–43	425 767.799	0.007	0.020	426 910.220	0.017	0.020
52–51	503 035.432	0.005	0.020	504 363.848	0.035	0.020
53–52	512 689.126	0.002	0.020	514 040.103	0.010	0.020
54–53	522 341.719	0.017	0.020	523 715.116	0.016	0.020
58–57			0.020	562 401.982	–0.009	0.020
59–58	570 587.097	–0.022	0.020	572 070.319	–0.012	0.020
60–59	580 232.584	0.004	0.020	581 737.272	–0.008	0.020
61–60	589 876.793	0.002	0.020			

^{a} Assumed uncertainty, see text; ^{b} from Brown et al. (1985).

for the overtone states. The spectra were analysed using Eqs. (1) and (2), and the previous cm-wave data for the $\upsilon_5 = 1$ state (Brown et al. 1985) were included in the corresponding data set with a reduced weighting factor ($w = 1/\sigma^2$), in order to take into account their lower measurement precision. Assumed uncertainties $\sigma = 20$ kHz and $\sigma = 100$ kHz were adopted for the present measurements and for the data of Brown et al. (1985), respectively. The complete list of the transition frequencies analysed for the states $\upsilon_5 = 1$, $\upsilon_5 = 2$ and $\upsilon_5 = 3$, and of the corresponding least-squares residuals are reported in Tables 3 and 4.

The least-squares fits yielded accurate values of the rotational and centrifugal distortion constants, including the sextic constant H, which was precisely determined for each state. Conversely, the octic centrifugal distortion constant L was kept fixed at the value determined for the ground state. The results of these least-squares fits are reported in Cols. 2–4 of Table 2.

Table 4. Analysed transition frequencies and least-squares residuals (MHz) for C_3O in the $v_5 = 2$ and $v_5 = 3$ bending overtone states.

Transition	Observed	O. – C.	Observed	O. – C.	Observed	O. – C.	Observed	O. – C.
	$v_5 = 2, l_5 = 0$		$v_5 = 2, l_5 = 2^-$		$v_5 = 2, l_5 = 2^+$			
9–8	87 943.091	0.011	87 944.878	0.000	87 951.218	–0.005		
10–9	97 711.921	–0.004	97 715.599	0.000	97 724.313	–0.004		
11–10	107 479.961	0.011	107 486.036	0.011	107 497.634	–0.006		
13–12	127 013.240	0.016	127 025.866	–0.014	127 045.062	0.006		
14–13	136 778.304	–0.013	136 795.255	0.006	136 819.176	–0.013		
34–33	331 759.467	–0.003	332 058.525	0.004	332 373.212	0.000		
35–34	341 489.182	–0.010	341 813.337	0.010	342 153.457	–0.002		
36–35	351 216.968	0.002	351 567.133	–0.004	351 933.659	0.003		
37–36	360 942.793	–0.014	361 319.960	0.034	361 713.726	–0.008		
38–37	370 666.735	–0.001	371 071.664	–0.004	371 493.622	0.004		
39–38	380 388.782	0.004	380 822.326	–0.010	381 273.230	–0.004		
40–39	390 108.966	0.004	390 571.894	–0.011	391 052.499	0.000		
41–40	399 827.329	0.011	400 320.340	–0.009	400 831.338	0.006		
	$v_5 = 3, l_5 = 1^-$		$v_5 = 3, l_5 = 3^-$		$v_5 = 3, l_5 = 3^+$		$v_5 = 3, l_5 = 1^+$	
9–8	88 369.449	0.002	88 614.291[a]	–0.008[b]	88 614.291[a]	–0.008[b]	88 866.759	0.003
10–9	98 186.646	0.001	98 459.883[a]	–0.009[b]	98 459.883[a]	–0.009[b]	98 738.955	0.013
11–10	108 003.341	0.008	108 305.369[a]	0.023[b]	108 305.369[a]	0.023[b]	108 610.532	0.006
13–12	127 634.989	0.002	127 995.623	–0.001	127 995.932	–0.003	128 351.630	–0.013
14–13	137 449.856	–0.004	137 840.489	–0.016	137 840.950	–0.006	138 221.062	0.009
34–33	333 547.176	–0.003	334 660.929	0.009	334 697.763	0.006	335 344.258	–0.017
35–34	343 339.384	–0.006	344 495.922	–0.008	344 538.309	–0.001	345 181.974	–0.011
36–35	353 130.196	0.002	354 330.138	0.014	354 378.663	–0.006	355 017.417	–0.008
37–36	362 919.579	0.007	364 163.482	0.016	364 218.833	–0.006	364 850.531	0.005
38–37	372 707.501	–0.001	373 995.911	–0.006	374 058.838	0.011	374 681.227	0.009
39–38	382 493.961	–0.005	383 827.436	–0.002	383 898.642	0.002	384 509.446	0.015
40–39	392 278.950	0.003	393 657.986	–0.004	393 738.277	–0.005		
41–40	402 062.427	0.000	403 487.521	–0.013	403 577.760	0.001	404 158.152	–0.001

Notes. – Assumed uncertainties are 20 kHz for all the transitions. [a] Unresolved *l*-doublet; [b] deviation between the experimental frequency of a blend of unresolved lines and the mean value of the corresponding calculated frequencies.

4. Discussion

This paper extends to the submm-wave region the study of the rotational spectra of C_3O in its ground vibrational state and, additionally, reports new mm-wave and submm-wave measurements for three vibrationally excited states of the v_5 bending manifold lying below 400 cm^{-1}. The fairly high J-values reached in the present investigation made possible an accurate analysis of the centrifugal distortion effects, resulting in the determination of the sextic constant H for all the vibrationally excited states and also of the octic constant L for the ground state. The l-type resonance effects ware taken into account in the analysis of the bending excited state spectra in order to obtain spectroscopic parameters with clear physical meaning. Indeed, the rotational and centrifugal distortion constants fitted for the overtone bending states $v_5 = 2$ and $v_5 = 3$ are in very good agreement with the values extrapolated from the singly excited bending state $v_5 = 1$.

In his theoretical work, Botschwina (2005) suggested that C_3O is a rather floppy molecule: on the basis of ab initio calculations he estimated a ratio between ground state and equilibrium centrifugal distortion constants D_0/D_e of 1.46, and adopted this parameter as an indicator of molecular floppiness. Our experimental results provide a confirmation of this hypothesis as: (i) the value of the sextic centrifugal distortion constant H is one order of magnitude higher than those of typical semirigid linear molecules containing four first-row atoms, such as HC_3N (Thorwirth et al. 2000) or HC_4H (Bizzocchi & Degli Esposti 2008); (ii) the octic centrifugal distortion constant L gave non negligible contributions to the frequencies of transitions with $J > 40$ and had to be included in the analysis of the ground state spectra, which span the largest J range; and (iii) both D and H centrifugal distortion constants exhibit a large vibrational dependence on the v_5 bending quantum number, undergoing changes of 30% and 90%, respectively, for a single excitation. This latter effect accounts for most of the unusually large D_0/D_e ratio (Botschwina 2005).

The improved set of spectroscopic constants derived in the present investigation allows the calculation of a very reliable set of rest frequencies for the lowest vibrationally excited states of C_3O at millimetre and submillimetre wavelengths. The predicted 1σ uncertainties do not exceed 30 kHz up to 800 GHz (0.01 $km\,s^{-1}$) for ground state lines, whereas for the excited state spectra the uncertainties are less than 50 kHz up to 500 GHz (0.03 $km\,s^{-1}$).

Tables 5–8, available in electronic form at the CDS, collect a list of rest frequencies between 10 GHz and 800 GHz calculated from the spectroscopic data of Table 2, including also the estimated uncertainty at the 1σ level of each transition as determined statistically by the least-squares fits (Albritton et al. 1976). The corresponding Einstein A-coefficients for spontaneous emission from state J' to J can be calculated for each line using (Herzberg 1950)

$$A_{J'\to J} = \frac{16\pi^3}{3\epsilon_0 h c^3}\frac{\nu^3_{J'J}}{2J'+1}L(J',l)|\mu|^2, \tag{3}$$

where $\nu_{J'J}$ is the transition frequency, μ is the molecular dipole moment, whose experimental value is 2.391(5) D (Brown et al. 1983), and $L(J', l)$ is the Hönl-London factor for a P-branch $\Delta l = 0$ transition (Herzberg 1950):

$$L(J', l) = (J' + l)(J' - l)/J'. \tag{4}$$

The detection of C_3O toward the extreme carbon star IRC+10216 stressed the similarity between the chemistry taking place in cold dense clouds and in the circumstellar envelopes of C-rich AGB stars (Agúndez et al. 2008), and it also put forth the need for a revised chemical model of these objects. Also, a recent study of IRC+10216 based on infrared observations (Fonfría et al. 2008) has shown that the IR pumping due to the MIR and FIR continuum coming from the dusty envelope is very effective in producing high non-LTE vibrational temperatures. Thus, the detection of vibrationally excited C_3O in IRC+10216 might provide useful information in understanding the mechanism of formation of O-bearing species in C-rich circumstellar envelopes.

Acknowledgements. This work has been supported by MIUR (PRIN 2005 funds, project "Trasferimenti di energia e di carica a livello molecolare") and by the University of Bologna (RFO funds).

References

Agúndez, M., & Cernicharo, J. 2006, ApJ, 650, 374

Agúndez, M., Cernicharo, J., Pardo, J. R., et al. 2008, Ap&SS, 313, 329

Albritton, D. L., Schmeltekopf, A. L., & Zare, R. N. 1976, Molecular Spectroscopy: Modern Approach II (New York: Academic Press), 1

Bizzocchi, L., & Degli Esposti, C. 2004, ApJ, 614, 518

Bizzocchi, L., & Degli Esposti, C. 2008, to be published

Botschwina, P. 2005, J. Mol. Struct. Theochem, 724, 95

Brown, R. D., Eastwood, E. W., Elmes, P. S., & Godfrey, P. D. 1983, J. Am. Chem. Soc., 105, 6496

Brown, R. D., Godfrey, P. D., Elmes, P. S., Rodler, M., & Tack, L. M. 1985, J. Am. Chem. Soc., 107, 4112

Cernicharo, J., Guélin, M., & Kahane, C. 2000, A&AS, 142, 181

Fonfría, J. P., Cernicharo, J., Richter, M. J., & Lacy, J. H. 2008, ApJ, 673, 445

Ford, K. E. S., Neufeld, D. A., Goldsmith, P. F., & Melnick, G. J. 2003, ApJ, 589, 430

Ford, K. E. S., Neufeld, D. A., Schilke, P., & Melnick, G. J. 2004, ApJ, 614, 990

Hasegawa, T. I., Kwok, S., Koning, N., et al. 2006, ApJ, 637, 791

Herzberg, G. 1950, Molecular spectra and molecular structure I. Spectra of diatomic molecules (USA: Krieger, Malabar FL)

Hochlaf, M. 2001, J. Mol. Spectrosc., 210, 284

Klebsch, W., Bester, M., Yamada, K. M. T., et al. 1985, A&A, 152, L12

Matthews, H. E., Irvine, W. M., abd R. D. Brown, P. F., & Godfrey, P. D. 1984, Nature, 310, 125

McNaughton, D., McGilvery, D., & Shanks, F. 1991, J. Mol. Spectrosc., 149, 458

Melnick, G. J., Neufeld, D. A., Ford, K. E. S., Hollenbach, D. J., & Ashby, M. L. N. 2001, Nature, 412, 160

Niederhoff, M., & Yamada, K. M. T. 1993, J. Mol. Spectrosc., 157, 182

Palumbo, M. E., Leto, P., Siringo, C., & Trigilio, C. 2008, ApJ preprint

Tang, T. B., Inokuchi, H., Saito, S., Yamada, C., & Hirota, H. 1985, Chem. Phys. Lett., 116, 83

Tenenbaum, E. D., Apponi, A. J., Ziurys, L. M., et al. 2006, ApJ, 649, L17

Thorwirth, S., Müller, H. S. P., & Winnewisser, G. 2000, J. Mol. Spectrosc., 204, 133

Tsuji, T. 1973, A&A, 23, 411

Yamada, K. M. T., Birss, F. W., & Aliev, M. R. 1985, J. Mol. Spectrosc., 112, 347

Yamada, K. M. T., Degli Esposti, C., Botschwina, P., et al. 2004, A&A, 425, 767